*R*esearch in
*A*stronomy and
*A*strophysics

Electric resistivity of partially ionized plasma in the lower solar atmosphere

Jongchul Chae[1] and Yuri E. Litvinenko[2]

[1] Astronomy Program, Department of Physics and Astronomy, Seoul National University, Seoul 08826, Korea; *jcchae@snu.ac.kr*

[2] Department of Mathematics, University of Waikato, P. B. 3105, Hamilton 3240, New Zealand

Abstract The lower solar atmosphere is a gravitationally stratified layer of partially ionized plasma. We calculate the electric resistivity in the solar photosphere and chromosphere, which is the key parameter that controls the rate of magnetic reconnection in a Sweet-Parker current sheet. The calculation takes into account the collisions between ions and hydrogen atoms as well as the electron-ion collisions and the electron-hydrogen atom collisions. We find that under the typical conditions of the quiet Sun, electric resistivity is determined mostly by the electron-hydrogen atom collisions in the photosphere, and mostly by the ion-hydrogen collisions, i.e. ambipolar diffusion, in the chromosphere. In magnetic reconnection events with strong magnetic fields, the ambipolar diffusion, however, may be insignificant because the heating by the reconnection itself may lead to the full ionization of hydrogen atoms. We conclude that ambipolar diffusion may be the most important source of electric resistivity responsible for the magnetic flux cancelation and energy release in chromospheric current sheets that can keep a significant fraction of neutral hydrogen atoms.

Key words: plasmas — atomic processes — magnetohydrodynamics (MHD) — Sun: atmosphere — Sun: chromosphere

1 INTRODUCTION

It is well known that magnetic reconnection occurs not only in the solar corona, but also in the lower solar atmosphere. In the solar corona, plasma is fully ionized and temperature is very high, and hence the classical electric resistivity is extremely low. Moreover, because of low mass density, plasma is collisionless in nature. Thus it was not possible to explain the fast rate of reconnection inferred from solar flares in terms of a current sheet model of Sweet-Parker type (Parker 1963), which required the development of models for fast reconnection such as Petschek reconnection (Petschek 1964).

By contrast, the plasma density in the low solar atmosphere is high enough for the plasma to be collisional, which has important consequences. Different particle species can be characterized by a single temperature. Electric resistivity is much higher than in the corona because temperature is low. The resistivity is further enhanced by the presence of neutral particles (Cowling 1957). As a matter of fact, in partially ionized plasma, electric resistivity is caused not only by the collisions between electrons and ions, but also by the collisions between electrons and neutral particles. Moreover, the phenomenon of ambipolar diffusion (or ion-neutral drift) in magnetized plasma can further increase the resistivity.

The electric resistivity enhanced by the presence of neutral particles is crucial for understanding magnetic reconnection occurring in the solar photosphere and chromosphere. The observed "cancelation" of adjacent magnetic flux tubes of opposite polarity has been regarded as an observable manifestation of Sweet-Parker magnetic reconnection in the photosphere and chromosphere (e.g., Litvinenko 1999; Sturrock 1999). The reconnection model incorporated the effects of compressibility of the current sheet plasma, and the rate of flux cancelation was included as an important parameter of magnetic reconnection (Chae et al. 2003; Litvinenko & Chae 2009). The Sweet-Parker current sheet models in these studies, however, were not fast enough to quantitatively explain the convergence speeds of the canceling magnetic features in the photosphere. Therefore alternative possibilities were also explored, including Petschek reconnection in the low atmosphere (Chae et al. 2002), the effect of flux pileup on the Sweet-Parker type reconnection (Litvinenko et al.

2007) and anomalous resistivity (Chae et al. 2003; Chae 2007). In all these studies, the electric resistivity enhanced by the presence of neutral particles was not taken into account. Accordingly, there is a good possibility that the effect of ambipolar diffusion on the resistivity, if included with the previously studied effects in the Sweet-Parker model, may explain the fast magnetic reconnection implied by the observed flux cancelations.

The theoretical investigation of magnetic reconnection in partially ionized plasmas started a few decades ago mainly in the context interstellar clouds (Zweibel 1989; Brandenburg & Zweibel 1994; Malyshkin & Zweibel 2011). As for magnetic reconnection occurring in the solar chromosphere, much theoretical progress was made during the last decade (see Ni et al. 2020, for review). Using multi-fluid simulations, Leake et al. (2012, 2013) demonstrated that the decoupling of neutral and ion fluids can eventually lead to a fast magnetic reconnection rate in the solar chromosphere. However, the later studies of Ni et al. (2015) and Ni & Lukin (2018) indicated that fast magnetic reconnection develops as a result of plasmoid instability, and the ambipolar diffusion has little effect on this process. This result may be applicable to the jet-like events displaying high temperature excess and high speeds observed in solar active regions such as the chromospheric anemone jets observed with the Solar Optical Telescope/Hinode (Singh et al. 2012a), the hot explosions observed by the Interface Region Imaging Spectrograph (IRIS) usually called IRIS bombs (Peter et al. 2014), and frequent jets from sunspot light bridges (Tian et al. 2018). This plasmoid-instability driven fast reconnection in the chromosphere is very similar to the fast magnetic reconnection in the corona that was theoretically studied to explain X-ray jets (Yokoyama & Shibata 1994), and solar flares (e.g., Bhattacharjee et al. 2009; Bárta et al. 2011), and was reported from observations (Lin et al. 2005; Takasao et al. 2012; Singh et al. 2012b). The efficiency of plasmoid-instability in magnetic reconnection in a general context was hence theoretically studied in depth (e.g., Loureiro et al. 2007). Note that the above plasmoid-instability driven model applies to magnetic reconnection occurring in the chromosphere of strong magnetic field regions such as solar active regions. In regions of weaker magnetic fields on the quiet Sun, however, there is a possibility that a model of Sweet-Parker type with an enhanced electric resistivity may explain fast reconnection, and so it is quite worth further investigation.

Ohm's law including ambipolar diffusion was previously derived (Cowling 1957; Braginskii 1965; Kubat & Karlicky 1986). Electric conductivity including ambipolar diffusion was also calculated in the solar atmosphere by Kubat & Karlicky (1986), Wang (1993) and Khomenko &

Collados (2012), and its effect was studied in the context of Sweet-Parker magnetic reconnection (Ni et al. 2007), as well as the plasma heating and electric current decay (Khomenko & Collados 2012). Among these calculations of electric conductivity, the work of Kubat & Karlicky (1986) appears to be the most comprehensive. They formulated the problem using Branginskii coefficients (Braginskii 1965) and presented a table of electric conductivities calculated as functions of height based on a specific atmospheric model: Model C of Vernazza et al. (1981). While the values in the table are very useful while studying the effects of ambipolar diffusion under the physical conditions specified in the model atmosphere, those values have only limited applicability if the physical conditions in a chromospheric feature significantly deviate from the model atmosphere.

Motivated by these considerations, in the present work we revisit the derivation of Ohm's law including the effects of neutral particles and the calculation of electric resistivity under realistic physical conditions of the solar chromosphere. Our work is intended to contribute to better quantifying the effect of electric resistivity on the rate of magnetic reconnection under different physical conditions of the chromosphere. We present a brief independent step-by-step derivation of Ohm's law in order to clarify the underlying physics and the approximations utilized for the derivation. We also present a practical way of calculating each contribution to the electric resistivity under arbitrary physical conditions of the chromosphere, generalizing the calculation previously performed for the standard model atmosphere. Finally, we also discuss the accuracy of our method and we investigate a numerical discrepancy between our results and those by Kubat & Karlicky (1986).

2 METHOD

2.1 Generalized Ohm's Law and Electric Resistivity

Ohm's law including ambipolar diffusion was treated in previous studies (Cowling 1957; Braginskii 1965; Kubat & Karlicky 1986). We begin by deriving Ohm's law from the three-fluid equations. While not new, a brief step-by-step derivation is necessary in order to clearly state the assumptions and approximations required for the derivation and thus justify a quantitative comparison of our results with those obtained previously. Note that the usual purpose of Ohm's law is to obtain the expression of an electric conductivity tensor to relate the electric field vector $\boldsymbol{E}'$ measured in the frame of plasma at rest and the electric current vector $\boldsymbol{j}$ (e.g., Cowling 1957; Sturrock 1994). Here we are primarily interested in the energy dissipation rate. Hence we do not derive the conductivity tensor, but rather directly derive the scalar electric resistivity η_e defined by

the equation

$$\boldsymbol{E}' \cdot \boldsymbol{j} = \eta_e j^2 \,. \tag{1}$$

As a matter of fact, the inverse of this resistivity is called the Cowling conductivity (Cowling 1957).

We assume that the plasma consists of free electrons of mass m_e and charge $-e$, singly-ionized ions of mass m_i and charge e, and neutral particles of mass m_n and zero charge. Electron fluid, ion fluid and neutral particle fluid, respectively, have number density n_e, n_i and n_n, mass density ρ_n, ρ_i and ρ_n, fluid velocity $\boldsymbol{v}_e$, $\boldsymbol{v}_i$ and $\boldsymbol{v}_n$, and pressure p_e, p_i and p_n. If all the ions are singly ionized, the condition for electrical neutrality leads to

$$n_e = n_i \,. \tag{2}$$

The generalized Ohm's law is derived from the momentum equation of electron fluid

$$\begin{aligned} \frac{\partial \rho_e \boldsymbol{v}_e}{\partial t} &+ \nabla \cdot (\rho_e \boldsymbol{v}_e \boldsymbol{v}_e) + \nabla p_e - \rho_e \boldsymbol{g} = \\ &- n_e e(\boldsymbol{E} + \frac{\boldsymbol{v}_e}{c} \times \boldsymbol{B}) - n_e \nu_{ei} m_{ei}(\boldsymbol{v}_e - \boldsymbol{v}_i) \\ &- n_e \nu_{en} m_{en}(\boldsymbol{v}_e - \boldsymbol{v}_n) \,, \end{aligned} \tag{3}$$

that of ion fluid

$$\begin{aligned} \frac{\partial \rho_i \boldsymbol{v}_i}{\partial t} &+ \nabla \cdot (\rho_i \boldsymbol{v}_i \boldsymbol{v}_i) + \nabla p_i - \rho_i \boldsymbol{g} = \\ &n_i e(\boldsymbol{E} + \frac{\boldsymbol{v}_i}{c} \times \boldsymbol{B}) - n_i \nu_{ie} m_{ie}(\boldsymbol{v}_i - \boldsymbol{v}_e) \\ &- n_i \nu_{in} m_{in}(\boldsymbol{v}_i - \boldsymbol{v}_n) \,, \end{aligned} \tag{4}$$

and that of neutral particle fluid

$$\begin{aligned} \frac{\partial \rho_n \boldsymbol{v}_n}{\partial t} &+ \nabla \cdot (\rho_n \boldsymbol{v}_n \boldsymbol{v}_n) + \nabla p_n - \rho_n \boldsymbol{g} = \\ &- n_n \nu_{ne} m_{ne}(\boldsymbol{v}_n - \boldsymbol{v}_e) \\ &- n_n \nu_{ni} m_{ni}(\boldsymbol{v}_n - \boldsymbol{v}_i) \,. \end{aligned} \tag{5}$$

The collisional frequency ν_{ei}, for instance, refers to the inverse of the time it takes for an electron to effectively lose its initial momentum by a series of collisions with ions. The mass m_{ei}, for instance, is the reduced mass of the two-body collision between electron and ion, which is given by $m_e m_i/(m_e + m_i)$. Note that m_{ei} is equal to m_{ie} and can be approximated to m_e because $m_e \ll m_i$. For the same reason, we have $m_{en} = m_{ne} \approx m_e$.

It is commonly assumed that the collisions are elastic where the total momentum does not change during the collisions. This assumption leads to the relationships:

$$n_e \nu_{ei} m_{ei} = n_i \nu_{ie} m_{ie} \,, \tag{6}$$
$$n_e \nu_{en} m_{en} = n_n \nu_{ne} m_{ne} \,, \tag{7}$$
$$n_i \nu_{in} m_{in} = n_n \nu_{ni} m_{ni} \,, \tag{8}$$

that justify the usefulness of Branginskii's coefficient of friction defined as, for instance, $\alpha_{ei} = n_e \nu_{ei} m_{ei}$ (Braginskii 1965).

By introducing the density, velocity, pressure and electric current density of the plasma fluid:

$$\rho \equiv \rho_e + \rho_i + \rho_n \simeq \rho_i + \rho_n \,, \tag{9}$$
$$\boldsymbol{v} \equiv \frac{\rho_e \boldsymbol{v}_e + \rho_i \boldsymbol{v}_i + \rho_n \boldsymbol{v}_n}{\rho_e + \rho_i + \rho_n} \simeq \frac{\rho_i \boldsymbol{v}_i + \rho_n \boldsymbol{v}_n}{\rho_i + \rho_n} \,, \tag{10}$$
$$p \equiv p_e + p_i + p_n \,, \tag{11}$$

and by adding the above three momentum equations, we obtain the momentum equation of the plasma fluid

$$\frac{\partial \rho \boldsymbol{v}}{\partial t} + \nabla \cdot \rho \boldsymbol{v}\boldsymbol{v} + \nabla p - \rho \boldsymbol{g} = \frac{\boldsymbol{j}}{c} \times \boldsymbol{B} \tag{12}$$

under the assumption

$$\rho_e \boldsymbol{v}_e \boldsymbol{v}_e + \rho_i \boldsymbol{v}_i \boldsymbol{v}_i + \rho_n \boldsymbol{v}_n \boldsymbol{v}_n \simeq \rho \boldsymbol{v}\boldsymbol{v} \,, \tag{13}$$

that holds under the conditions $|\boldsymbol{v}_i - \boldsymbol{v}| \ll |\boldsymbol{v}|$ and $|\boldsymbol{v}_n - \boldsymbol{v}| \ll |\boldsymbol{v}|$.

For the derivation of Ohm's law, we ignore the electron inertia and set the left-hand side of the electron momentum Equation (3) to zero

$$\frac{\partial \rho_e \boldsymbol{v}_e}{\partial t} + \nabla \cdot (\rho_e \boldsymbol{v}_e \boldsymbol{v}_e) + \nabla p_e - \rho_e \boldsymbol{g} = 0 \,, \tag{14}$$

which leads to the equation

$$\begin{aligned} \frac{\partial \rho_i \boldsymbol{v}_i}{\partial t} &+ \nabla \cdot (\rho_i \boldsymbol{v}_i \boldsymbol{v}_i) + \nabla p_i - \rho_i \boldsymbol{g} \\ &\simeq (1 - f) \left[\frac{\partial \rho \boldsymbol{v}}{\partial t} + \nabla \cdot \rho \boldsymbol{v}\boldsymbol{v} + \nabla p - \rho \boldsymbol{g} \right] \\ &= (1 - f)\frac{\boldsymbol{j}}{c} \times \boldsymbol{B} \,, \end{aligned} \tag{15}$$

where f is the mass fraction of neutral particles

$$f \equiv \frac{\rho_n}{\rho} \,, \tag{16}$$

which is assumed to be constant over local space and local time.

By adding Equations (3) and (4) and by making use of Equation (15), we obtain

$$\begin{aligned} (1 - f)\frac{\boldsymbol{j}}{c} \times \boldsymbol{B} = \frac{\boldsymbol{j}}{c} \times \boldsymbol{B} &- n_e \nu_{en} m_{en}(\boldsymbol{v}_e - \boldsymbol{v}_n) \\ &- n_i \nu_{in} m_{in}(\boldsymbol{v}_i - \boldsymbol{v}_n) \,. \end{aligned} \tag{17}$$

Here we adopt the assumption that the magnitude of $n_e \nu_{en} m_{en}(\boldsymbol{v}_e - \boldsymbol{v}_n)$ is much smaller than that of $n_i \nu_{in} m_{in}(\boldsymbol{v}_i - \boldsymbol{v}_n)$. This assumption holds because $m_{en} \ll m_{in}$ whereas ν_{en} is of the same order of magnitude as ν_{in} (as will be shown in the next section), and $|\boldsymbol{v}_e - \boldsymbol{v}_n|$ is expected to be comparable to $|\boldsymbol{v}_i - \boldsymbol{v}_n|$ (because $|\boldsymbol{v}_e - \boldsymbol{v}_i|$ may be much smaller than $|\boldsymbol{v}_i - \boldsymbol{v}_n|$ because of tighter coupling between electrons and ions). With this simplifying assumption, it is useful to define two

drift velocities $\boldsymbol{v}_{ei} \equiv \boldsymbol{v}_e - \boldsymbol{v}_i$ and $\boldsymbol{v}_{in} \equiv \boldsymbol{v}_i - \boldsymbol{v}_n$. Note that $\boldsymbol{v}_{ei}$ is directly related to the current density

$$\boldsymbol{v}_{ei} = -\frac{\boldsymbol{j}}{n_e e}, \tag{18}$$

and Equation (17) leads to the expression

$$\boldsymbol{v}_{in} \simeq \frac{f}{n_i \nu_{in} m_{in}} \frac{\boldsymbol{j}}{c} \times \boldsymbol{B}. \tag{19}$$

From Equations (3) and (14), we obtain

$$\boldsymbol{E} = -\frac{\boldsymbol{v}_e}{c} \times \boldsymbol{B} - \frac{(\nu_{ei} + \nu_{en})m_e}{e} \boldsymbol{v}_{ei} \\ - \frac{\nu_{en} m_e}{e} \boldsymbol{v}_{in}, \tag{20}$$

and by inserting the expression of $\boldsymbol{v}_e$ written in terms of $\boldsymbol{v}$, $\boldsymbol{v}_{ei}$ and $\boldsymbol{v}_{in}$

$$\boldsymbol{v}_e = \boldsymbol{v} + f\boldsymbol{v}_{in} + \boldsymbol{v}_{ei} \tag{21}$$

into the above equation, we obtain the equation

$$\boldsymbol{E}' \equiv \boldsymbol{E} + \frac{\boldsymbol{v}}{c} \times \boldsymbol{B} \\ = -\frac{(\nu_{ei} + \nu_{en})m_e}{e} \boldsymbol{v}_{ei} - \frac{\nu_{en} m_e}{e} \boldsymbol{v}_{in} \\ - \frac{f\boldsymbol{v}_{in}}{c} \times \boldsymbol{B} - \frac{\boldsymbol{v}_{ei}}{c} \times \boldsymbol{B} \tag{22}$$

expressed in terms of the drift velocity $\boldsymbol{v}_{ei}$ and $\boldsymbol{v}_{in}$. By utilizing Equations (18) and (19), we obtain the generalized Ohm's law

$$\boldsymbol{E}' = \frac{(\nu_{ei} + \nu_{en})m_e}{n_e e^2} \boldsymbol{j} + \frac{f^2 B^2}{n_i \nu_{in} m_{in} c^2} \boldsymbol{j}_\perp \\ + \left(1 - f\frac{n_e \nu_{en} m_e}{n_i \nu_{in} m_{in}}\right) \frac{1}{n_e e c} \boldsymbol{j} \times \boldsymbol{B} \tag{23}$$

expressed in $\boldsymbol{j}$. Here $\boldsymbol{j}_\perp \equiv \boldsymbol{j} - (\boldsymbol{j} \cdot \boldsymbol{B})\boldsymbol{B}/B^2$ is the component of the current density vector perpendicular to the magnetic field. In principle, from this form of Ohm's law one can derive the expression of the electric conductivity tensor. But in the present work, we are interested in the derivation of a scalar electric resistivity that quantifies the energy release rate in plasma. By taking the scalar product of both sides of this equation and $\boldsymbol{j}$, we obtain the expression for the work done by electric force on the plasma

$$\boldsymbol{E}' \cdot \boldsymbol{j} = \left[\frac{\nu_{ei} m_e}{n_e e^2} + \frac{\nu_{en} m_e}{n_e e^2} + \frac{f^2 B^2 \sin^2 \theta}{n_i \nu_{in} m_{in} c^2} \right] j^2, \tag{24}$$

where θ is the angle between $\boldsymbol{j}$ and $\boldsymbol{B}$, and we obtain the expression of electric resistivity

$$\eta_e = \eta_{ei} + \eta_{en} + \eta_{in} \tag{25}$$

with

$$\eta_{ei} = \frac{\nu_{ei} m_e}{n_e e^2},$$
$$\eta_{en} = \frac{\nu_{en} m_e}{n_e e^2}, \tag{26}$$
$$\eta_{in} = \frac{f^2 B^2 \sin^2 \theta}{n_i \nu_{in} m_{in} c^2}. \tag{27}$$

The physical meaning of η_{ei} and η_{en} is obvious. The term η_{ei} is related to the dissipation of electromagnetic energy by the collisions of electrons with ions. The second term η_{en} is related to the collisions of electrons and neutral particles. The last term η_{in} is a consequence of the ion slip, i.e. the difference between $\boldsymbol{v}_i$ and $\boldsymbol{v}_n$ that arises from the Lorentz force that the ions are subject to, but the neutral particles are not, and from the infrequent collisions between ions and neutral particles (Cowling 1957, see also Kunkel 1984 and references therein). Note that the Hall component, the last term on the right in Equation (23), does not contribute either to the dissipation of electromagnetic energy or to electric resistivity because it is perpendicular to $\boldsymbol{j}$. Note also that the Hall term appears to be affected by the ion slip, but this effect seems to be negligible because of the inequality $\nu_{en} m_e \ll \nu_{in} m_{in}$ mentioned above.

2.2 Calculation in the Low Solar Atmosphere

The three-fluid description above assumes that the plasma consists of three particle species: free electrons, neutral particles and ions. Real plasma in the low solar atmosphere, however, consists of a number of different species of particles. We consider four species only – free electrons, protons, neutral hydrogen atoms and hypothetical metal ions whereas Kubat & Karlicky (1986) considered nine species including helium ions, and five kinds of metal ions. Basically we assume that all the ions are singly ionized, so n_e is equal to n_i as in Equation (2). There are two major sources of electrons and ions: hydrogen atoms and metals, so we can write the number density of ions

$$n_e = n_p + n_M, \tag{28}$$
$$n_p = x_H n_H, \tag{29}$$
$$n_M = A_M n_H. \tag{30}$$

The notation is as follows: n_p, the number density of protons, n_M, the number density of metal ions, n_H, the number density of all hydrogens (hydrogen atoms and protons), x_H, the ionization fraction of hydrogen and, A_M, the number ratio of metallic ions to hydrogens. We regard hydrogen atoms as the only species of neutral particles that is important in the collisions with either electrons or ions, so we can write

$$n_n = n(H_0) = (1 - x_H)n_H, \tag{31}$$
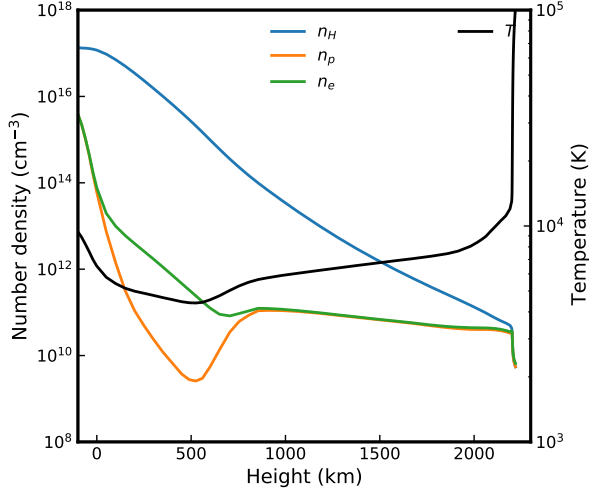
Fig. 1 Height variations of temperature and number densities of all hydrogens, protons and electrons in the FAL-C model.

$$f = 1 - x_H \,, \qquad (32)$$

and

$$\nu_{en} = \nu_{eH} \,. \qquad (33)$$

Meanwhile, two kinds of collisions contribute to η_{in}: the collisions between protons and neutral hydrogens specified by the subscript $_{pH}$ and the collisions between metal ions and neutral hydrogens specified by the subscript $_{MH}$. Therefore we write

$$n_i \nu_{in} m_{in} = n_p \nu_{pH} m_{pH} + n_M \nu_{MH} m_{MH} \,. \qquad (34)$$

The calculation of η_{ei}, η_{en} and η_{in} requires the values of n_e, n_n, n_i, f, $B\sin\theta$ as well as T. Note that n_e, n_n, n_i and f are fully specified if x_H, A_M as well as n_H are given. Figure 1 presents the height variations of n_H, n_e and n_p in the FAL-C model (Fontenla et al. 1993). The FAL-C model is the revision of the VAL-C model, Model C of Vernazza et al. (1981). The FAL-C model took into account the effect of particle diffusion on the formation of hydrogen lines and helium lines and hence does not display any ad hoc temperature plateau in the transition region unlike the VAL-C model. We will adopt the FAL-C model for the investigation of electric resistivity in the quiet Sun chromosphere, but will rely on the VAL-C model for comparison with the previous calculation of Kubat & Karlicky (1986).

It can be seen from the figure that n_p is much smaller than n_e around the temperature minimum region, indicating the major source of electrons is not hydrogen atoms, but metals. The value of A_M is bigger than x_H only around the temperature minimum region. For simplicity we set A_M to a constant value of 1.2×10^{-4}, that is very close to the minimum of n_i/n_H. The value of x_H can be directly

taken from the atmospheric model or can be calculated utilizing the equation of ionization equilibrium

$$x_H = f(n_e, T, R_{ik}) \qquad (35)$$

as described by Chae (2021) when the photoionization rate R_{ik} is given.

We employ two alternative methods for calculating the electric resistivity, depending on how x_H and other quantities are specified.

– Method 1: The value of x_H as well as n_H and T is taken from the reference atmospheric model like the VAL-C model (Vernazza et al. 1981) or the FAL-C model (Fontenla et al. 1993). This method is straightforward to implement, but cannot be applied to the plasma having thermodynamic parameters different from the model.

– Method 2: The values of two independent parameters (e.g., p and T) and R_{ik} are given. The values of x_H and the other quantities are derived with the help of auxiliary equations

$$p = n_H(1 + x_H + A_{He})k_B T \,, \qquad (36)$$
$$\rho = n_H(1 + 4A_{He})m_H \,, \qquad (37)$$

as well as the equations above. We set the abundance of helium A_{He} to 0.1. This method can be applied to plasma having arbitrary thermodynamic parameters.

2.3 Collisional Frequencies

Suppose the cross-section $\sigma_{\alpha\beta}(w)$ of an α particle and a β particle is known given the relative speed w. Then the inverse of the time for an α particle to collide with β particles effectively once is given by

$$\nu_{\alpha\beta} = n_\beta \frac{1}{3} \int \sigma_{\alpha\beta}(w) \frac{w^3}{\sigma_w^2} f_0(\boldsymbol{w}) d\boldsymbol{w} \,, \qquad (38)$$

where it is assumed that the relative velocity $\boldsymbol{w}$ follows a Maxwellian distribution where the magnitude of the mean $\langle \boldsymbol{w} \rangle$ is much smaller than the standard deviation $\sigma_w \equiv (kT/m_{\alpha\beta})^{1/2}$.

The cross-section of a Coulomb collision between an electron and a singly-ionized ion is known (e.g., Sturrock 1994) to be

$$\sigma_{ei} = 4\pi \left(\frac{e^2}{m_e w^2} \right)^2 \lambda_{ei} \,, \qquad (39)$$

with the Coulomb logarithm λ_{ei} given by

$$\lambda_{ei} = 23 - \ln \left(n_e^{1/2} T_{eV}^{-3/2} \right) \qquad (40)$$

within the temperature range of $T_{\text{eV}} < 10$ where T_{eV} refers to temperature in unit of eV. It thus follows

$$\nu_{ei} = \frac{4}{3}\left(\frac{2\pi}{m_e}\right)^{1/2}\frac{e^4}{(k_B T)^{3/2}}n_i\lambda_{ei} \tag{41}$$
$$= 2.9\times10^{-6}\ \text{s}^{-1}T_{\text{ev}}^{-3/2}n_i\lambda_{ei}\,,$$

where n_i is in the unit of cm^{-3}.

The cross-section of collision with neutral particles can be modeled as a hard sphere collision where the cross-section is independent of the relative speed, and the collisional frequency is expressed as

$$\nu_{\alpha\beta} = n_\beta\sigma_{\alpha\beta}\frac{4}{3}\left(\frac{8kT}{\pi m_{\alpha\beta}}\right)^{1/2}. \tag{42}$$

Note that in the lower solar atmosphere, the neutral particles are practically hydrogen atoms. The ions are practically protons except near the temperature minimum region, where the ions are metal ions. We use the collisional cross-section between an electron and a hydrogen atom

$$\sigma_{eH} = 35\pi a_0^2 = 3.1\times10^{-15}\ \text{cm}^2 \tag{43}$$

that was taken by Kubat & Karlicky (1986) where $a_0 = 5.3\times10^{-9}$ cm is the Bohr radius.

We also utilize the cross-section of collision between a proton and a hydrogen atom

$$\sigma_{pH} = 217g(T)\pi a_0^2 = 19\times10^{-15}g(T)\ \text{cm}^2 \tag{44}$$

taken from table 5 of Hunter & Kuriyan (1977). The factor $g(T)$ is equal to 1 when $T_{\text{ev}} \equiv T/11604 = 0.5$, and decreases from 1.15 to 0.57 in the energy range of T_{ev} from 0.1 to 10 eV. We also note that $m_{eH} \simeq m_e$ and $m_{pH} = m_H/2$.

Near the temperature minimum region, hydrogen is hardly ionized at all, and hence protons are a minor species. The sources of the ions and electrons are the elements with very low first ionization potential and with relatively high abundance, which include Al, Na, Ca and Fe. We model the different kinds of ions originating from these elements by a hypothetical metal ion. The cross-section of a collision between this metal ion and a hydrogen atom is modeled by the formula

$$\sigma_{MH} = (r+1)^2\sigma_{pH}\,, \tag{45}$$

where r is the classical radius ratio of the ion to the hydrogen atom, which we set to 3. Note that $m_{MH} \simeq m_H$. Thus we have

$$\nu_{eH} = 2.8\times10^{-7}\ \text{s}^{-1}T_{\text{ev}}^{1/2}n(H_0)\,, \tag{46}$$
$$\nu_{pH} = 5.6\times10^{-8}\ \text{s}^{-1}g(T)T_{\text{ev}}^{1/2}n(H_0)\,, \tag{47}$$
$$\nu_{MH} = 6.3\times10^{-7}\ \text{s}^{-1}g(T)T_{\text{ev}}^{1/2}n(H_0)\,, \tag{48}$$

where $n(H_0)$ is the number density of hydrogen atoms. Note that ν_{eH} and ν_{pH} are indeed of the same order of magnitude, as we assumed earlier.
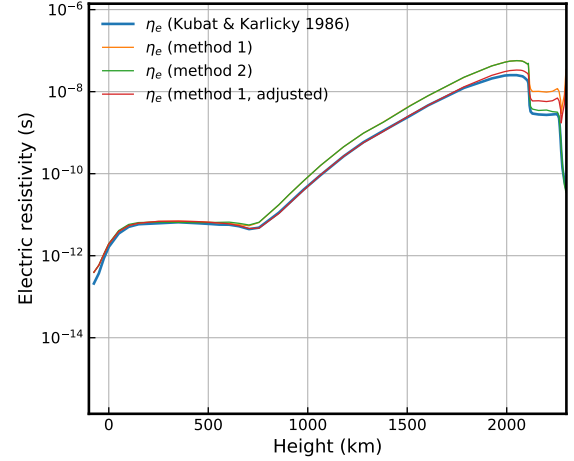
Fig. 2 Height variations of electric resistivity. For comparison with Kubat & Karlicky (1986), we adopted the VAL-C model and $B\sin\theta = 100$ G.

3 RESULTS

We calculated η_e following the above-described methods and compared the results with those of Kubat & Karlicky (1986). We adopted the VAL-C model like Kubat & Karlicky (1986). Figure 2 indicates that at heights below 2100 km where hydrogen is not fully ionized, there is no significant difference between the two methods we employed, supporting the validity of method 2 calculating the electric resistivity from two independent thermodynamic parameters and the photoionization rate of hydrogen. Our calculations, however, produce systematically larger values of η_e than the calculation of Kubat & Karlicky (1986). This discrepancy seems to arise from the difference in the adopted value of σ_{pH}. We directly took the values given in the table of Hunter & Kuriyan (1977), but Kubat & Karlicky (1986) computed σ_{pH} by integrating the graphs of differential cross-sections presented by Hunter & Kuriyan (1980). In principle, this integration should yield the same value as the table of Hunter & Kuriyan (1977), because those results were based on the same work done by the same authors. Since Kubat & Karlicky (1986) did not specify the total cross-section they obtained from the integration, we cannot directly compare our choice with that of Kubat & Karlicky (1986). If we adjust this parameter by multiplying it by 1.7, we can obtain the values of resistivity that are in good agreement with those of Kubat & Karlicky (1986). Nevertheless, we do not employ such adjustment in the present work since this adjustment is not physically justified.

It can be seen from Figure 3 that ν_{ei}, ν_{eH} and ν_{pH} in the low solar atmosphere (FAL-C model) are very high ($> 10^3$ s^{-1}). This means that the plasma is fully collisional, achieving dynamical relaxation among particles of different species on time scales shorter than
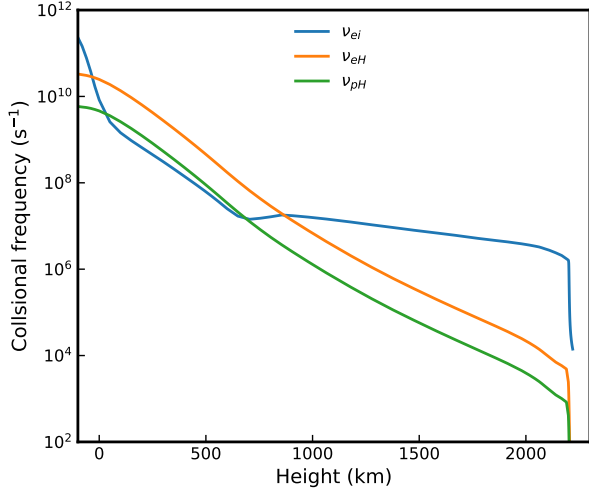
Fig. 3 Height variations of collisional frequencies calculated with the FAL-C model.
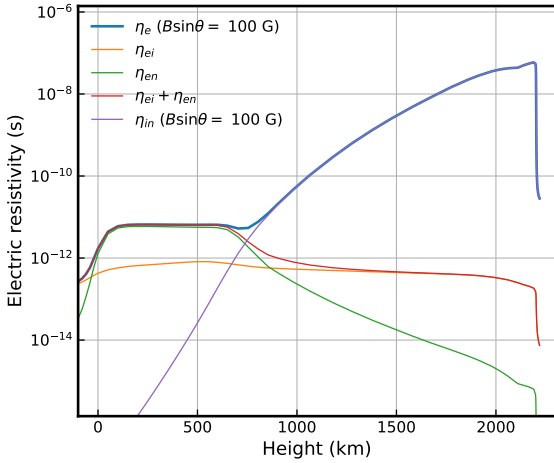
Fig. 4 Height variations of electric resistivity based on the FAL-C model with $B \sin \theta = 100$ G.

10^{-3} s. As a result, we can conclude that all of the electron fluid, ion fluid and neutral particle fluid have the same temperature in the low solar atmosphere. Specifically, we find that ν_{ei} decreases from 1×10^{10} s^{-1} at height 0 km to 1×10^{6} s^{-1} at height 2200 km, ν_{eH}, from 3×10^{10} s^{-1} to 5×10^{3} s^{-1}, and ν_{pH}, from 5×10^{9} s^{-1} to 8×10^{2} s^{-1}. These height variations mostly reflect those of n_i and $n(H_0)$ to which the collisional frequencies are proportional.

Figure 4 displays the height variations of electric resistivity η_e in the low solar atmosphere in the specific case of $B \sin \theta = 100$ G. It ranges from 2×10^{-12} s at height 0 km to 6×10^{-8} s at height 2200 km. The dominant contribution comes from η_{en} at heights < 750 km and from η_{in} at heights > 750 km. This means that the collisions with neutral particles are the most important source of electric resistivity in the low solar atmosphere. Note that

the term η_{en} is proportional to n_n/n_e since $\nu_{en} \propto n_n$. This term increases when the particles are less ionized. Meanwhile, η_{in} is proportional to $(1 - x_H)/((x_H + A_M)n_H^2)$. As long as x_H is smaller than 1, η_{in} increases with height because n_H rapidly decreases with height. But at heights $> 22\,000$ km, x_H rapidly approaches 1 and so η_{in} rapidly decreases with height.

Figure 4 also demonstrates that the contribution of η_{ei} to η_e is minor. The resistivity contribution η_{ei} coincides with the Spitzer resistivity in a fully-ionized plasma (Spitzer 1956). Because $\nu_{ei} \propto n_i$ and $n_i = n_e$, the low temperature of the low solar atmosphere is preferential for a high value of η_{ei}. Nevertheless, its value is found to be smaller than either η_{en} or η_{in} throughout the low solar atmosphere. Particularly at heights > 1000 km, η_{in} overwhelms $\eta_{ei}+\eta_{en}$ with the ratio $\eta_{in}/(\eta_{ei}+\eta_{en})$ ranging from 80 at height 1000 km to 3×10^5 at height 2200 km. Note for clarity that the value of this ratio is proportional to the square of $B \sin \theta$. If we choose a smaller value $B \sin \theta = 10$ G instead of 100 G, the ratio will have a range of smaller values from 1 to 3×10^3. However, it is very likely that $B \sin \theta > 10$ G in solar chromospheric features, and so we conclude that η_{in} dominates the electric resistivity in such features.

4 DISCUSSION

The electric resistivity η_e is the key parameter that controls the rate of magnetic reconnection in a Sweet-Parker current sheet. Motivated by the requirements of quantitative modeling of observable reconnection features in the solar chromosphere, we have revisited the calculation of η_e and compared the results with those of Kubat & Karlicky (1986). We presented two methods for calculating the electric resistivity η_e in the low solar atmosphere when the physical conditions are specified. The results are in good agreement with the tabulated values of $1/\sigma_C$ presented by Kubat & Karlicky (1986) except for the discrepancy arising from uncertainty in the cross-section of proton-hydrogen collision they used. We emphasize that our second method can be employed even when the solar plasma is not described by the VAL-C model, thus extending the earlier results.

Our results clearly indicated that η_{in} may significantly exceed η_{ei} in the solar chromosphere. In the middle chromosphere at height 1500 km, the value of η_{in} is roughly 100 times that of $\eta_{ei} + \eta_{en}$ in the case of $B \sin \theta = 10$ G. The large electric resistivity associated with the ion-hydrogen atom collisions in chromospheric plasma with a neutral component fully resolves the problem that a fast rate of magnetic reconnection cannot be achieved in a Sweet-Parker current sheet when only the resistivity arising from the electron-ion collisions and

electron-hydrogen atom collisions is considered. Because of this problem, Chae et al. (2003) and Chae (2007) introduced an ad hoc anomalous resistivity, corresponding to a resistivity enhancement by a factor of order of 100. The resistivity arising from the ion-hydrogen collisions can be the physical cause of the enhanced resistivity in the solar chromosphere if there exist a large enough number of neutral hydrogen atoms.

Physically, η_{in}, or ambipolar diffusion, comes into play only when electric currents are flowing in the direction perpendicular to the magnetic field. This is because η_{in} is directly related to the ion-neutral drift velocity $\boldsymbol{v}_{in}$, and this velocity is basically driven by the Lorentz force acting on ions. The value of η_{in} becomes zero in the force-free magnetic configuration where the Lorentz force is zero. An electric current sheet is such a structure where electric currents flow perpendicular to magnetic fields. In this kind of structure, η_{in} becomes important. An interesting thing is that the formation of sharp structures like current sheets can be driven by ambipolar diffusion itself because of the anisotropic nature of ambipolar diffusion (Brandenburg & Zweibel 1994).

There exist two situations of astrophysical interest where the electric current flows perpendicular to magnetic field: Alfvén waves and current sheets. As an illustration, we estimate the values of $\boldsymbol{j}$, $\boldsymbol{v}_{ei}$ and $\boldsymbol{v}_{in}$ in these two cases. Specifically we will consider Alfvén waves and current sheets that might exist in the chromosphere at a height of 1600 km. We obtain from the FAL-C model: $\rho = 2.3 \times 10^{-12}$, $n_e = 6.3 \times 10^{10}$, $x_H = 0.06$ and $\nu_{ei} = 7. \times 10^6$ s^{-1}, $\nu_{pH} = 3.4 \times 10^4$ s^{-1}. If we choose $B = 50$ G, the Alfvén speed is found to be $c_A = 93$ km s^{-1}.

We first consider the Alfvén waves that have a velocity amplitude of $v_0 = 10$ km s^{-1} and period $P = 150$ s or angular frequency $\omega = 0.04$ rad s^{-1}. The amplitude of the alternating electric current associated with the Alfvén waves is then given by

$$j_0 = \frac{cB\omega v_0}{4\pi c_A^2} = 60 \text{ statA cm}^{-2} \qquad (49)$$
$$= 2 \times 10^{-4} \text{ A m}^{-2}.$$

Based on this value, the electron-proton drift speed v_{ei} is estimated at 1.9 cm s^{-1}, and the ion-neutral drift speed v_{in} at 51 cm s^{-1}. These speeds are much lower than the plasma velocity v_0.

Now we consider a current sheet characterized by $\delta B = 50$ G and $l = 10$ km. The electric current density in this current sheet is given

$$j = \frac{c\delta B}{4\pi\delta l} = 1.2 \times 10^5 \text{ statA cm}^{-2} \qquad (50)$$
$$= 0.4 \text{ A m}^{-2},$$

which is much larger than the estimate for the Alfvén waves in the above. The electron-ion drift speed v_{ei} in this current sheet is estimated at 0.04 km s^{-1}, and the corresponding ion-neutral speed v_{in} at 1.0 km s^{-1}. Note that this value of v_{in} is of the same order as the speed of plasma inflowing into the current sheet (e.g., Chae et al. 2003).

Our results indicate that the ion-neutral drift velocity is an important source of electric resistivity that controls the rate of magnetic reconnection and energy release in current sheets in the solar chromosphere. This conclusion holds for the current sheets containing a significant number of hydrogen atoms. Note, however, that the process of magnetic reconnection itself heats plasma in the current sheet and causes more hydrogen atoms to get ionized, resulting in the decrease of hydrogen atoms and η_{in}. Whether η_{in} is important in these events or not depends on how much neutral hydrogens are left in the current sheets.

For example, Ellerman bombs, the well-known magnetic reconnection events in the chromosphere of active regions, are known to accompany the temperature increase of several hundred to several thousand K (e.g., Fang et al. 2006; Hong et al. 2017), and to have temperature of 7000 to 9000 K (e.g., Danilovic 2017). Very recently, Chae (2021) investigated the ionization of hydrogen in the solar chromosphere by adopting the photoionization rate inferred from the FALC model, and concluded that plasma features contain more than 10% neutral hydrogen at temperatures lower than 17 000 K, but less than 1% neutral hydrogen at temperatures higher than 23 000 K. This result suggests that the Ellerman bombs can contain a significant fraction of neutral hydrogen atoms. The fraction of neutral hydrogen possibly decreases a bit in a dynamic atmosphere by the dynamic ionization that is more affected by the high temperature phase (Carlsson & Stein 2002). Nevertheless, it is very likely that the Ellerman bombs still contain enough neutral hydrogens, which is the reason why they are observed well through the Hα line. Accordingly, it seems quite worthwhile to investigate the effect of η_{in} on magnetic reconnection in charge of Ellerman bombs. However, the recently discovered ultraviolet (UV) bursts (Peter et al. 2014; Young et al. 2018), often called IRIS bombs, may be different. These events usually take place around and above the temperature minimum region and the temperature in the UV burst region may be higher than 20 000 K because they are observed through the UV emission lines of ions existing at transition region temperatures. Therefore, it is very likely that hydrogen is almost fully ionized in UV bursts, leading to $\eta_{en} = \eta_{in} = 0$. In this situation, the fast rate of magnetic reconnection cannot be achieved in a Sweet-Parker current sheet and may have to be explained by an alternative mechanism,

such as the plasmoid-instability driven reconnection model of Petschek type (e.g., Ni et al. 2015).

We conclude that η_{in} can explain the fast rate of magnetic reconnection when the temperature increase in the current sheet is not large enough to significantly increase hydrogen ionization. This is the case for the early phase of magnetic reconnection with strong magnetic fields in solar active regions (e.g., Ni et al. 2015) or for the magnetic reconnection of weak fields on the quiet Sun. In the future, we intend to incorporate the results of our calculation of the electric resistivity into our model of compressible reconnection in a Sweet-Parker current sheet (Chae 2007; Litvinenko & Chae 2009). Our intention is to take into account ambipolar diffusion, ionization and recombination of hydrogen, as well as a realistic energy equation and time-dependent effects, in order to obtain results that can quantitatively describe the magnetic flux cancelation observed in the solar photosphere.

References

Bárta, M., Büchner, J., Karlický, M., & Skála, J. 2011, ApJ, 737, 24

Bhattacharjee, A., Huang, Y.-M., Yang, H., & Rogers, B. 2009, Physics of Plasmas, 16, 112102

Braginskii, S. I. 1965, Reviews of Plasma Physics, 1, 205

Brandenburg, A., & Zweibel, E. G. 1994, ApJL, 427, L91

Carlsson, M., & Stein, R. F. 2002, ApJ, 572, 626

Chae, J., Choi, B.-K., & Park, M.-J. 2002, Journal of Korean Astronomical Society, 35, 59

Chae, J., Moon, Y.-J., & Park, S.-Y. 2003, Journal of Korean Astronomical Society, 36, S13

Chae, J. 2007, in Astronomical Society of the Pacific Conference Series, New Solar Physics with Solar-B Mission, 369, 243

Chae, J. 2021, Journal of Astronomy and Space Sciences, 38, 83

Cowling, T. G. 1957, Magnetohydrodynamics (New York: Interscience)

Danilovic, S. 2017, A&A, 601, A122

Fang, C., Tang, Y. H., & Xu, Z., et al. 2006, ApJ, 643, 1325

Fontenla, J. M., Avrett, E. H., & Loeser, R. 1993, ApJ, 406, 319

Hong, J., Ding, M. D., & Cao, W. 2017, ApJ, 838, 101

Hunter, G., & Kuriyan, M. 1977, Proceedings of the Royal Society of London Series A, 353, 575

Hunter, G., & Kuriyan, M. 1980, Atomic Data and Nuclear Data Tables, 25, 287

Khomenko, E., & Collados, M. 2012, ApJ, 747, 87

Kubat, J., & Karlicky, M. 1986, Bulletin of the Astronomical Institutes of Czechoslovakia, 37, 155

Kunkel, W. B. 1984, Physics of Fluids, 27, 2369

Leake, J. E., Lukin, V. S., Linton, M. G., & Meier, E. T. 2012, ApJ, 760, 109

Leake, J. E., Lukin, V. S., & Linton, M. G. 2013, Physics of Plasmas, 20, 061202

Lin, J., Ko, Y.-K., et al. 2005, ApJ, 622, 1251

Litvinenko, Y. E. 1999, ApJ, 515, 435

Litvinenko, Y. E., Chae, J., & Park, S.-Y. 2007, ApJ, 662, 1302

Litvinenko, Y. E., & Chae, J. 2009, A&A, 495, 953

Loureiro, N. F., Schekochihin, A. A., & Cowley, S. C. 2007, Physics of Plasmas, 14, 100703

Malyshkin, L. M., & Zweibel, E. G. 2011, ApJ, 739, 72

Ni, L., Yang, Z., & Wang, H. 2007, Ap&SS, 312, 139

Ni, L., Kliem, B., Lin, J., & Wu, N. 2015, ApJ, 799, 79

Ni, L., & Lukin, V. S. 2018, ApJ, 868, 144

Ni, L., Ji, H., Murphy, N. A., & Jara-Almonte, J. 2020, Proceedings of the Royal Society of London Series A, 476, 20190867

Parker, E. N. 1963, ApJS, 8, 177

Peter, H., Tian, H., Curdt, W., et al. 2014, Science, 346, 1255726

Petschek, H. E. 1964, NASA Special Publication, 50, 425

Singh, K. A. P., Isobe, H., Nishida, K., & Shibata, K. 2012a, ApJ, 760, 28

Singh, K. A. P., Isobe, H., Nishizuka, N., et al. 2012b, ApJ, 759, 33

Spitzer, L. 1956, Physics of Fully Ionized Gases (New York: Interscience)

Sturrock, P. A. 1994, Plasma Physics (Cambridge: Cambridge Univ. Press)

Sturrock, P. A. 1999, ApJ, 521, 451

Takasao, S., Asai, A., Isobe, H., & Shibata, K. 2012, ApJL, 745, L6

Tian, H., Yurchyshyn, V., Peter, H., et al. 2018, ApJ, 854, 92

Vernazza, J. E., Avrett, E. H., & Loeser, R. 1981, ApJS, 45, 635

Wang, J. 1993, in IAU Colloq. 141: The Magnetic and Velocity Fields of Solar Active Regions, 46, 465

Yokoyama, T., & Shibata, K. 1994, ApJL, 436, L197

Young, P. R., Tian, H., Peter, H., et al. 2018, Space Sci. Rev., 214, 120

Zweibel, E. G. 1989, ApJ, 340, 550